Hydrologic Modeling with NEXRAD Precipitation in Middle Tennessee

V. S. Neary, M.ASCE[1]; E. Habib[2]; and M. Fleming, M.ASCE[3]

Abstract: The use of radar-based precipitation is investigated for possible improvement of spatially lumped continuous hydrologic modeling in two subbasins of the Cumberland River basin in Middle Tennessee. Hydrologic predictions of streamflow at the outlets of the subbasins are obtained using HEC-HMS and two precipitation inputs, Stage III radar-derived and gauge-only data. Model performance with each precipitation input is assessed by comparing predicted and measured streamflow at each subbasin outlet and calculating streamflow volume bias, root mean square difference, mean normalized peak error, and mean peak timing error. The results indicate that the Stage III precipitation suffers from systematic underestimation at both the point and subbasin scales and cannot be completely offset by model recalibration. Simulations driven by both the Stage III and gauge-only data periodically failed to reproduce observed flood peaks in both subbasins. But Stage III simulations are generally less accurate in prediction of streamflow volume as compared to gauge-only simulations and, although comparable to the gauge-only simulations in predicting the magnitude and time to peak, offer no apparent improvement in predicting these quantities either.

DOI: 10.1061/(ASCE)1084-0699(2004)9:5(339)

CE Database subject headings: Hydrologic models; Flood hydrology; Hydrologic data; Precipitation; Streamflow forecasting; Tennessee.

Introduction

Among various input data to hydrologic models, precipitation measurements arguably have the most critical influence on the hydrologic model's performance. Traditionally, hydrologic models have relied on point gauge measurements to provide the required precipitation data. However, for lumped hydrologic modeling applications, areal-averaged precipitation information is needed. Therefore, precipitation estimates from gauges become inadequate due to their poor representation of areal precipitation, especially in situations with sparse gauge network arrangements (Rodriguez-Iturbe and Mejia 1974; Morrissey et al. 1995). Alternatively, weather radar that covers much larger spatial areas has become an attractive instrument for providing average areal precipitation information. Despite its indirect means of measuring precipitation, radar represents a significant improvement over gauges because it resolves the natural variability of precipitation over temporal and spatial scales that are relevant to hydrologic applications. Therefore, it has been a common belief by the hydrologic community that the use of detailed radar estimates is expected to improve the accuracy of hydrologic model simulations and forecasts. In recent years, the potential value of high-resolution radar data was explored using synthetically simulated radar precipitation fields or estimates from actual radar observations. However, despite numerous studies that addressed this issue, mixed—and sometimes contradicting—results were often reported. Some studies investigated the effect of spatial and temporal variability of precipitation on the accuracy of the simulated hydrographs (Krajewski et al. 1991; Ogden and Julien 1994; Chaubey et al. 1999), while others have emphasized the importance of correct representation of total precipitation volumes (Beven and Hornberger 1982). Bedient et al. (2000) indicated that radar data resulted in flood predictions as accurate as the rain gauge data. Sun et al. (2000) indicated that, without the use of optimal estimation methods, radar data could result in errors greater than those associated with gauge observations. Preliminary analysis by Johnson et al. (1999) showed a comparable performance of radar and gauge with some instances of erroneous results in the case of radar-based simulation. Results from Obled et al. (1994) showed that using distributed rainfall information did not lead to improved hydrograph simulations. Complexities such as dependence on model type (lumped versus distributed or semidistributed), catchment size, runoff-generation mechanism [saturation-excess versus infiltration-excess (Winchel et al. 1998)], and quality of radar data and its estimation algorithms (Sun et al. 2000) make it difficult to draw any general conclusions about the value of radar data to improve the results of hydrologic models.

In recent years, the National Weather Service (NWS) has installed the NEXRAD (Next Generation Weather Radar) system, which consists of a national network of radars known as WSR-88D (Weather Surveillance Radar–1988 Doppler). Regional NWS River Forecasting Centers (RFC) generate the Stage III hourly 4×4 km^2 precipitation products in support of operational hydrologic forecasting using the NEXRAD system products and

[1]Associate Professor, Dept. of Civil and Environmental Engineering, Tennessee Technological Univ., Cookeville, TN. E-mail: vsneary@tntech.edu

[2]Assistant Professor, Dept. of Civil and Environmental Engineering, Univ. of Louisiana at Lafayette, Lafayette, LA. E-mail: habib@louisiana.edu

[3]Hydraulic Engineer, U.S. Army Corps of Engineers, Hydrologic Engineering Center, Davis, CA.

Note. Discussion open until February 1, 2005. Separate discussions must be submitted for individual papers. To extend the closing date by one month, a written request must be filed with the ASCE Managing Editor. The manuscript for this paper was submitted for review and possible publication on May 28, 2003; approved on December 19, 2003. This paper is part of the ***Journal of Hydrologic Engineering***, Vol. 9, No. 5, September, 2004. ©ASCE, ISSN 1084-0699/2004/5-339–349/$18.00.

gauge data. The fact that Stage III data provide detailed spatial precipitation information makes it an attractive candidate to replace gauges as input to hydrologic simulations. In an effort to take advantage of the increasingly available radar data, several federal agencies (e.g., the U.S. Army Corps of Engineers, the U.S. Environmental Protection Agency, the U.S. Department of Agriculture, and the National Weather Service) have modified their hydrologic models so that radar data can be utilized. One of the recent hydrologic modeling software to utilize radar-based precipitation information is the Hydrologic Modeling System (HMS) program developed by the Hydrologic Engineering Center (HEC) of the U.S. Army Corps of Engineers (HEC 2000). HEC-HMS is widely used for hydrologic modeling, forecasting, and water budget studies. Currently, the Corps of Engineers Nashville District is using HMS as a tool for flood forecasting and water budget analyses in the Cumberland River basin. Traditionally, rain gauge data has been used in HEC-HMS and HEC-1 simulations and only preliminary investigations (McNutt and Neary 1999) have examined the use of radar data.

This study investigates the value of using operational radar-based precipitation information for possible improvement of spatially lumped continuous hydrologic modeling in two subbasins of the Cumberland River basin. The study compares hydrologic simulations using HEC-HMS and two precipitation inputs: the Stage III radar products and the gauge observations. Because it is recognized that the accuracy of streamflow prediction is largely dependent on the quality of the driving precipitation input (whether from radar or gauges), the current study performs an extensive evaluation of the accuracy of the radar data before using it as input to the HEC-HMS simulations. This paper is organized as follows. First, a description of the study site and the available data is presented. Detailed analysis of the uncertainty of the radar data is then performed at two spatial scales: the 4×4 km^2 radar pixel scale and the basin scale. Results of the hydrologic simulations are presented and statistical measures are used to examine the model performance with the radar data as compared to that with the gauge data. The paper closes with conclusions and recommendations for improving the radar product and radar-based hydrologic simulations.

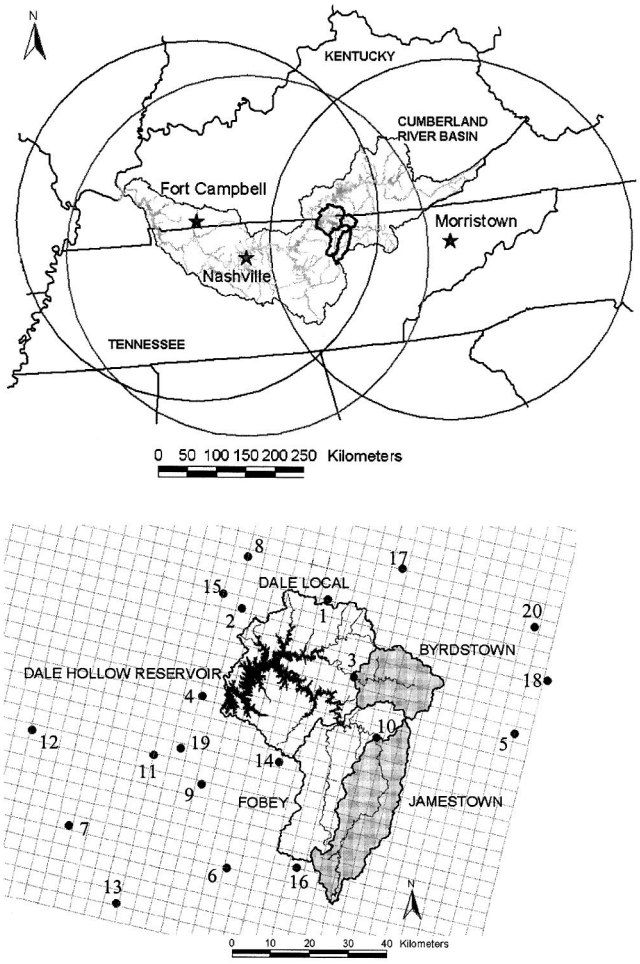

Fig. 1. Study site: Upper map shows the Cumberland River Basin with the 250 km umbrellas of the three NEXRAD radars at Nashville, Fort Campbell, and Morristown. Lower map shows the subbasins of the Dale Hollow watershed. Rain gauges inside and nearby the watershed are shown as circles. The squares represent the 4×4 km^2 radar HRAP grid.

Study Site

The Dale Hollow watershed has an approximate area of 2,424 km^2 and is located within the Cumberland River basin, as shown in Fig. 1. The watershed includes the Obey and Wolf River systems. The Dale Hollow reservoir, originally intended for flood control and hydropower, is now managed for water quality, water supply, fish and wildlife habitat, and recreation. The average annual rainfall over the watershed is 1,455.4 mm and the average annual snowfall is 355.6 mm. Elevations in the watershed range from 154 m (at the dam) to 622 m. For this study, the Dale Hollow watershed is divided into five subbasins in accordance with the existing Corps hydrologic models: Byrdstown, Jamestown, Fobey, Dale Local, and Pool. The Byrdstown and Jamestown subbasins are approximately 275 and 550 km^2 in area, respectively. They are gauged at their outlets, allowing for model calibration and validation at interior nodes within the Dale Hollow watershed. Hourly streamflow measurements for the Byrdstown and Jamestown subbasins, processed by the U.S. Geological Survey (USGS), were available from the Nashville District, U.S. Army Corps of Engineers (USACE) for the study period 1997–2001. Hourly gauge and radar data were also available. A detailed description and analysis of this data will be presented in the following sections. Average monthly evapotranspiration input was obtained from the National Oceanic and Atmospheric Administration (NOAA) Web site: http://cdo.ncdc.noaa.gov/plclimprod/plsql/poemain.poe.

Evaluation of Radar Products

Precipitation Data

Two sets of hourly precipitation data are available for the current study: gauge observations and radar-gauge estimates. Gauge data were collected from 20 recording gauges located in the vicinity of the Dale Hollow watershed and were provided by the Nashville District of the USACE for the study period 1997–2001. The spatial distribution of the gauges (Fig. 1) shows that no gauges are located inside the two subbasins of Byrdstown and Jamestown (for which hydrologic simulations will be performed) and only two gauges are located on their boundaries. The gauge density for the study watershed is about 0.0018 gauges/km^2. This density is comparable to the study by Johnson et al. (1999) and better than

the average density in the United States, which is approximately 0.0013 gauges/km^2 (Linsley et al. 1992). According to Bradley et al. (2002), at 0.0018 gauge/km^2, the study site gauge density herein will result in mean areal precipitation estimates with errors between 30 and 45%.

The quality of gauges can be suspect due to frequent breakdown caused by mechanical and electronic failure. Unfortunately, information about the quality of the gauges and how reliable their data are is not available for this study. To the extent possible, the gauge data were checked for quality by cross-comparison with nearby gauges and with the corresponding radar data to eliminate any observational periods that were highly questionable. Such periods were flagged and not included in any further analysis.

Radar estimates used in this study are the Stage III operational precipitation products of the NEXRAD system and were obtained from the National Weather Service (NWS) Ohio River Forecast Center (OHRFC). Stage III products are hourly accumulations of precipitation over a grid of approximately 4×4 km^2 that is usually referred to as an HRAP grid [Hydrologic Rainfall Analysis Project (Reed and Maidment 1999)]. Full descriptions of the Stage III products and its processing algorithms are available in numerous publications (e.g., Seo et al. 1997; Fulton et al. 1998) and only a brief description is provided herein. Development of Stage III data is a three-step process that starts from the raw radar reflectivity field (Z). In Stage I, a power law Z-R relationship is applied to estimate fields of precipitation rates, R, that are then integrated over time to produce hourly accumulations. The result of the Stage I process is the radar-only products known as digital precipitation products (DPA); an evaluation of the DPA products is available in Smith et al. (1996) and Seo et al. (1999). In Stage II, gauge observations are used to construct the mean field bias of the radar estimates (Seo et al. 1997), which is then used to produce bias-adjusted radar precipitation estimates over the HRAP cells. In addition, a gauge-only precipitation field is also produced over the HRAP grid and then optimally merged with the bias-adjusted radar field to produce the Stage II products. The final step involves the ''mosaicing'' of the Stage II products from the multiple radars to produce a single Stage III product over the OHRFC region.

It is well recognized that using radar systems to measure precipitation is subject to several sources of uncertainty (e.g., Austin 1987). The main source of uncertainty is attributed to the fact that radar does not measure rainfall in a direct way. It measures the quantity known as reflectivity Z, which is then converted into rainfall rate R through a preestablished Z-R relationship. The selection of a certain Z-R relationship, which is highly nonlinear, imposes significant uncertainty on the accuracy of the derived precipitation information. Another type of uncertainty is due to the fact that surface rainfall has to be deduced from radar measurements sampled at a certain height above the ground. Variability in the vertical profile of precipitation fields can cause significant overestimation or underestimation of the true surface precipitation rates. Other uncertainties arise from factors related to radar hardware calibration and radar sampling properties.

All of the aforementioned factors are expected to have a significant impact on the accuracy of the Stage III radar products and will consequently affect the performance of the hydrologic model; therefore, it is essential to evaluate the uncertainty of the input precipitation data before performing the hydrologic simulations. Due to the lack of information about the true surface precipitation amounts, uncertainty quantification efforts tend to rely on comparing concurrent and collocated radar and gauge rainfall estimates. However, this has proven to be problematic due to the differences in the temporal and spatial sampling properties between the two sensors (e.g., Austin 1987; Hitch 1991; Brandes et al. 1999; Wang et al. 2000). In the current study, the Stage III products are evaluated by comparison against the corresponding observations of the 20 gauges that are located in the study area. Radar 4×4 km^2 estimates are compared with individual gauges first, then basin-average radar and gauge estimates are compared. It should be mentioned that data from some of the 20 rain gauges available to the current study have been used by the OHRFC as part of the Stage III processing. In addition to being used in the removal of mean-field bias, gauge data are often used by hydrometeorological analysis and service (HAS) forecasters at the RFC to perform quality control on the generated Stage III products. In some instances where the original radar estimates are missing, data from the operational gauges are used instead. Therefore, some of the gauges available to this study do not represent an independent data source for validation of the Stage III products. An extensive effort was made to identify the set of gauges that have been used in the Stage III products so that they can be excluded from the comparison analysis. Unfortunately, information about these particular gauges, and the specific hours during which they were included in the radar data analysis, was not documented by the HAS forecasters. Nevertheless, information from such a long record of gauge observations can still be used to gain some insight about the quality of the radar data that are used in the hydrologic simulations.

Comparison with Individual Gauges

To evaluate the quality of the hourly 4×4 km^2 radar data, radar estimates were compared with the corresponding gauge observations. Concurrent hourly radar-gauge pairs for the period 1997–2001 are shown in the scatter plot in Fig. 2(a). The plotted pairs in the figure are for the radar pixels that contain gauges. The linear features apparent in the plot (instances of exact or close match of the radar and gauge values) are a result of the lack of independence between the two sets of estimates. As discussed earlier, gauge observations were used in the Stage III processing to adjust and sometimes replace the radar estimates. However, the main feature in this plot is the significant scatter at both low and high rain rates. Such scatter is not entirely attributed to the uncertainty in radar products. Two other sources of uncertainty are also responsible: (1) uncertainty in gauge observations caused by systematic effects (wind, splashing, evaporation, and mechanical and electronic malfunctioning) and random effects due to poor temporal sampling resolutions; and (2) uncertainty due to the difference in sampling areas of radar (4×4 km^2) and gauge (near point), which is usually referred to as point-area difference. Sorting out and quantifying the contribution of each uncertainty source is not straightforward. On the one hand, quantification of gauge errors was not possible in the current study due to lack of relevant information. However, other studies (e.g., Habib et al. 1999, 2001a,b) indicated that, except for malfunctioning, the magnitude of gauge errors could be neglected when hourly scale is considered. On the other hand, quantification of random errors, induced by the difference in sampling areas between radar and gauge, requires information about rainfall small-scale spatial variability (Ciach and Krajewski 1999; Habib and Krajewski 2002). To the best of the writers' knowledge, such information is not available for the Middle Tennessee region; therefore, assessment of this uncertainty component was not possible. Despite this ambiguity in error separation, some useful results can still be obtained from the radar-gauge comparisons. To assess the quality of

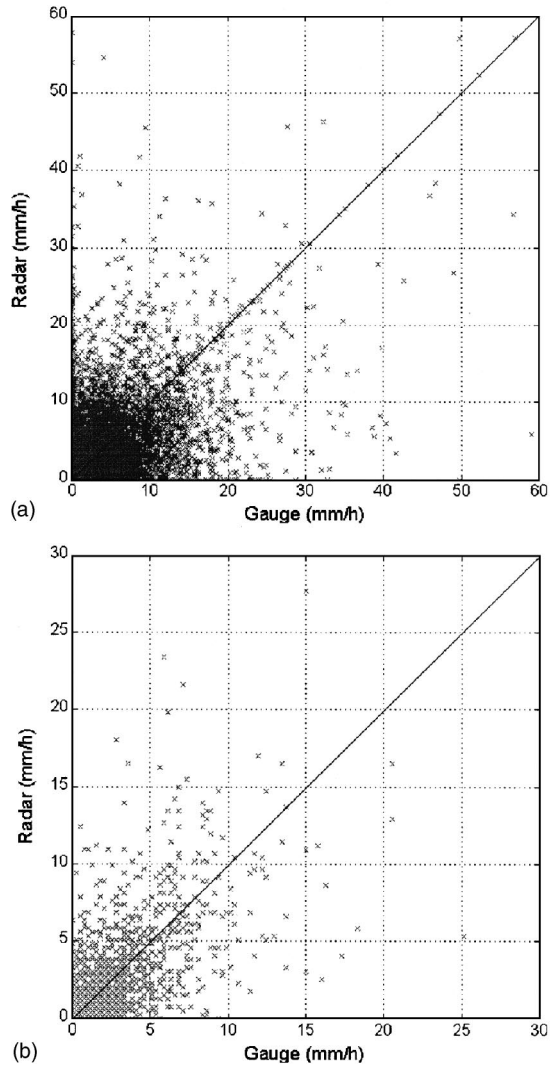

Fig. 2. Scatter plot of gauge and radar rainfall rates: (a) Single gauges and 4×4 km^2 radar pixels; (b) basin-average gauge estimates, BAG, and basin-average radar estimates, BAR

the radar estimates, two statistical measures, bias B_p and relative root mean square difference RMSD, are computed for the concurrent radar and gauge pairs

$$B_p(\%) = \frac{\overline{R} - \overline{G}}{\overline{G}} \cdot 100 \tag{1}$$

$$\mathrm{RMSD}(\%) = \frac{\sqrt{1/n \Sigma_{i=1}^{i=n} (R_i - G_i)^2 - (R-G)^2}}{\overline{G}} \cdot 100 \tag{2}$$

where G_i and R_i represent the ith hour precipitation rate of gauge and radar, respectively (mm/h); $\overline{G}$ and $\overline{R}$=mean values; and n=sample size of radar and gauge pairs. The preceding statistics were computed for each individual gauge. The results, along with other relevant information such as sample size and average gauge rain rate, are summarized in Table 1. It should be noted that the sample of each gauge site was constructed using only pairs that contained precipitation for either gauge or radar (i.e., only hours with either $G_i > 0$ or $R_i > 0$). By excluding pairs that have zero values for both radar and gauge, the sample constructed out of the period of 1997–2001 amounted to more than 45,000 hours for the 20 gauges combined. The sample shows that the average precipitation rate observed by the gauges was in the range of 1.3–2.0 mm/h.

Table 1. Statistical Analysis of Radar-Rainfall 4×4 km^2 Data Using Gauge Observations

Gauge number	Hours	$\overline{G}$ (mm/h)	B_p (%)	RMSD (%)	$P(G>0$ and $R=0)$	$P(R>0$ and $G=0)$
1	2,030	1.6	2.5	170.1	26.5	22.5
2	2,291	1.6	−3.1	182.9	29.2	19.0
3	2,828	1.5	−7.2	199.0	36.1	19.7
4	2,498	1.5	−1.6	210.4	30.0	22.5
5	2,879	1.4	−12.9	163.6	37.2	19.1
6	3,225	1.3	−11.5	200.5	46.1	16.2
7	2,265	1.4	8.8	164.9	28.7	20.1
8	2,552	1.5	−0.9	137.4	25.6	16.2
9	2,868	1.7	−21.8	167.0	36.2	17.9
10	2,776	1.5	−5.0	192.7	35.5	20.0
11	1,740	1.7	−8.5	227.9	33.6	25.7
12	2,481	2.0	−8.9	136.9	24.9	14.6
13	2,745	0.9	88.3	364.2	27.8	34.1
14	1,979	1.7	−9.3	128.0	25.3	16.9
15	2,186	1.2	38.3	271.9	18.2	50.3
16	2,586	1.8	−5.3	136.0	26.3	17.6
17	2,588	1.5	−8.7	153.5	32.1	17.9
18	2,609	1.4	−4.5	175.8	28.8	21.6
19	2,623	1.6	−4.3	225.2	35.0	19.4
20	2,352	1.3	−0.5	158.5	28.2	26.0
All gauges	45,170	1.5	−6.2	176.0	31.9	19.4
Maximum		2.0	8.8	227.9	46.1	26.0
Minimum		1.3	−21.8	128.0	24.9	14.6

Note: Statistics of gauges 13 and 15 are not included in computing statistics of all gauges, maximum, and minimum.

Before proceeding with analysis of the results, it should be noted that the statistics associated with gauges 13 and 15 are significantly different from the rest of the gauges and were not included in the statistical assessment. Close examination of individual observations of these two gauges showed several hours of nonfunctioning; therefore, they were not considered representative of the radar-gauge differences. Only two gauges show positive bias, while the rest of the gauges, with the exception of gauges 13 and 15, indicate that radar tends to be underbiased as compared to gauge precipitation. This agrees well with earlier studies that evaluated the accuracy of NEXRAD precipitation products (Smith et al. 1996; Young et al. 2000). The underestimation is in the range of −0.5 to −12.9% for most of the gauges, with one value reaching as high as −21.8%. When combining the samples of all gauges, the overall bias becomes −6.2%. This underestimation was unexpected, given the fact that some of the 20 gauges were used by the Stage III processing system to correct for the bias of the radar products.

While bias is a measure of systematic differences, the random differences between radar and gauges can be quantified by the relative root mean square difference that is computed as the standard deviation of differences normalized by their mean value. This statistic is always larger than 100% and reaches more than 200% for a few of the simulation periods. The combined sample of the 20 gauges has an RMSD value of 176. Such high values indicate that, besides the systematic underestimation bias, significant random differences exist between the radar products and the corresponding gauge observations. Another statistical measure is

Table 2. Analysis of Probability of Detection of Radar Rainfall Estimates for Single Gauges and 4×4 km^2 Radar Pixels, $P(R>0|G>g)$

g (mm/h)	$P(R>0\|G>g)$
0	60.3
1	80.3
2	85.8
5	89.7
10	89.7
15	92.0
20	91.8
30	94.2

the correlation coefficient between radar and gauge pairs; the values of this statistic are mostly in the range of 0.5–0.8. However, the correlation coefficient could be subject to significant overestimation problems caused by high skewness in the samples used (Habib et al. 2001a,b). Therefore, its value should be considered with caution.

Radar-gauge comparisons also revealed that, for numerous instances, a precipitation estimate from one sensor is zero when the other sensor's estimate is larger than zero. This is related to the ability of each sensor to successfully detect rainfall. To examine this issue, two probability ratios were computed: $P[R_i>0$ and $G_i=0]$, and $P[R_i=0$ and $G_i>0]$. The results are shown in Table 1 for each gauge. The occurrence of hours with ($R_i>0$ and $G_i=0$) can be justified, given the fact that the radar sampling area is much larger than that of the gauge (rainfall is known to be highly intermittent in space and time). However, the higher probability values reported with the case of ($R_i=0$ and $G_i>0$) indicate that radar products failed to detect rainfall for a significant number of hours. This may be attributed to factors such as overshooting of the radar beam (especially at far ranges) and quality control of the raw radar data. To examine whether the poor detection was associated with a certain range of rainfall intensities, the probability of the radar-rain detection was recalculated in a conditional sense: $P[R_i>0|G_i>g]$, where g=gauge precipitation rate. The results summarized in Table 2 show that the low detection probability is associated with low precipitation rates [similar behavior was reported by Young et al. (2000)]. However, even for high rates (20 mm/h and higher), radar still missed about 5% of rainy hours. Lack of information about the quality of gauge observations makes it difficult to confirm whether detection problems at such high precipitation rates are actually due to radar or gauge-related errors.

Comparison with Basin-Average Gauge Estimates

In this study, the hydrologic model simulations are performed using average precipitation input over the Byrdstown and Jamestown subbasins. Therefore, it is necessary to compare the basin-average radar precipitation estimates (BAR) versus the basin-average gauge estimates (BAG). It should be noted that, unlike individual gauge estimates, BAG estimates should be closer to the true areal precipitation over the subbasin areas. However, these improved estimates are still subject to uncertainty, because only a few gauges were used to obtain basin-average precipitation values. Quantifying the degree of uncertainty associated with a certain number of gauges, or how many gauges are needed to provide accurate estimates, is not possible due to the lack of information about small-scale rainfall variability (Bras and Rodriguez-Iturbe 1993; Morrissey et al. 1995). However, as mentioned previously, simulation-based analysis by Bradley et al. (2002) indicates errors as high as 45% with the study site gauge density. In the current analysis, BAR values are obtained by simple averaging of the HRAP pixels located inside each basin. For the BAG values, observations of individual gauges are first interpolated at each HRAP pixel, then averaged over the basin area. Interpolation was performed using the inverse-distance-squared method.

This study considers 21 simulation periods in the years between 1997 and 2001: 10 in spring seasons, four in summer seasons, and seven in winter seasons. The durations of these simulation periods range from 5 to 37 days. Many of the simulated periods contained multiple rainfall bursts. The periods were selected in such a way that considerable rainfall/streamflow quantities were observed. The total amounts of precipitation in each simulation period range from less than 50 mm to more than 250 mm. Before performing the hydrologic simulations, BAR estimates for each of the 21 periods were compared with the corresponding BAG estimates. This helps to gain insight about the quality of radar input data into the hydrologic model. A scatter plot of BAR versus BAG is shown in Fig. 2(b). The figure combines comparisons for all 21 simulations for the Byrdstown and Jamestown subbasins. Significant scatter characterizes the plotted pairs at both low and high rain rates. However, the scatter is less than that of the case of comparing the 4×4 km^2 radar estimates versus single gauges, as was shown in Fig. 2(a). Despite averaging gauge and radar estimates over the two subbasin areas (275 and 550 km^2), the scatter plot shows instances where the two precipitation estimates differ by as high as 15–20 mm/h.

Similar to the comparison of individual gauges, various statistics were computed to quantify the differences between basin-average radar and gauge estimates. The values of bias, RMSD, and probabilities of detection, along with the sample size and mean gauge precipitation, are summarized in Tables 4 and 5 for each simulation period and for the Byrdstown and Jamestown subbasins. Overall, the statistics of the two basins show similar behavior. The bias values show occurrences of both overestimation and underestimation. However, radar underestimation of gauge rainfall dominates most of the 21 periods. Out of the 21 simulation periods, underestimation is reported 14 times for Byrdstown and 17 times for Jamestown. The underestimation is mostly in the range of −10 to −20%, with three bias values exceeding −40%. Overestimation levels are generally less than 15%, with one value only exceeding 40%. When combined, the 21 simulation periods have an overall bias of −7.6% for Byrdstown and −14.1% for Jamestown, indicating that overall the radar BAR estimates tended to underestimate the gauge rainfall. Earlier studies (e.g., Johnson et al. 1999; Wang et al. 2000; Stellman et al. 2001) reported similar findings; however, bias values were different given that their analysis was based on different temporal and spatial scales (6-hour, daily, monthly, and 4×4 km^2) and different locations. The overall radar underestimation bias has significant implications for hydrologic modeling. After some duration, even small levels of underestimation bias lead to undesired drying of the model soil moisture (Smith et al. 1999); this will be further discussed in the following sections.

Tables 4 and 5 also show the values of the RMSD statistic that quantifies the random scatter in comparing BAR and BAG estimates. For most of the simulation periods, RMSD ranges between 100 and 150% for both Byrdstown and Jamestown, with a few periods exceeding 200%. Such large values indicate significant disagreement between hourly radar and gauge basin-average esti-

Table 3. Analysis of Probability of Detection for Basin-Average Gauge Estimates, BAG, and Basin-Average Radar Estimates, BAR, $P(R>0|G>g)$

g (mm/h)	$P(R>0\|G>g)$
0	59.9
1	86.3
2	94.4
3	97.2
4	98.6
5	98.8

mates. The analysis of the 4×4 km^2 radar estimates showed considerable detection problems, as indicated in Table 2. To examine whether such a problem exists with the basin-average estimates, the relevant conditional probabilities of detection are computed both conditionally and unconditionally. The results are summarized in Tables 3–5. For the 21 simulation periods combined, the probability of ($R=0$ and $G>0$) was quite large (38% for Byrdstown and 34.8% for Jamestown). The detection problem is more evident at low rainfall rates, as indicated in Table 3. Such lack of detection, both at the two scales of 4×4 km^2 and the basin area, is worrisome, because detection of precipitation is one of the main advantages behind using radar systems for observing precipitation. A general remark is that all the aforementioned statistics show the highest levels of disagreement between radar and gauge estimates (large bias, large RMSD, and poor detection ability) during simulation periods that were in cold months (November–March). This is expected, because the radar processing system and its estimation algorithms are known to be subject to more uncertainties during cold seasons (Hunter 1996; Super and Holroyd 1998). Generally, winter storms are more difficult to measure accurately due to several factors such as beam overshooting and variability in the vertical profiles of reflectivity (Seo and Johnson 1995).

HEC-HMS Simulations

The HEC-HMS model, with its soil-moisture-accounting (SMA) algorithm for continuous simulation (HEC 2000), was employed to compare streamflow simulations using BAG and BAR estimates. Excess rainfall was transformed to direct runoff at each subbasin outlet using the Clark unit hydrograph method (i.e., channel routing was not performed). Model parameter settings were guided by the detailed calibration and validation study of Fleming and Neary (2004). Given the underbias between the BAG and BAR precipitation products, it was necessary to calibrate the model for each precipitation product. Bradley and Kruger (1998) discuss the importance of model recalibration when switching precipitation products, particularly when an observed bias in precipitation is found between the two products. Indeed, this study confirmed that recalibration was required to improve the radar-driven simulation. It was also decided to calibrate the model for each of the 21 simulation periods in order to produce the best possible hydrologic simulations for each product—recognizing that this would not be done in a typical continuous hydrologic modeling application.

The SMA algorithm requires 12 parameters to model canopy storage, surface depression storage, soil storage, groundwater storage, surface runoff, interflow, and groundwater flow. The

Table 4. Statistical Parameters: Byrdstown

		Precipitation				Streamflow								
							B_v (%)		RMSD (%)		MNPE (%)		MPTE (h)	
Period	Hours	$\overline{G}$ (mm/h)	B_p (%)	RMSD (%)	$P(G>0$ and $R=0)$	$\overline{Q}_o$ (m^3/s)	G	R	G	R	G	R	G	R
2/24/97–3/10/97	360	2.3	−25.4	90.7	20.3	33.8	−10.0	−40.3	30.7	79.0	15.5	42.9	2.5	4.6
5/30/97–6/19/97	504	1.1	6.1	132.4	25.5	22.7	−14.6	−18.4	103.0	80.0	95.0	35.4	3.4	2.2
1/1/98–1/20/98	480	1.5	−19.0	111.2	48.8	11.8	9.9	9.3	64.7	51.2	69.9	10.9	4.0	4.3
2/1/98–2/26/98	624	0.7	−47.9	62.2	63.3	12.6	−28.7	−65.9	63.6	72.5	27.1	39.9	8.0	7.3
3/6/98–3/26/98	504	1.3	−22.2	104.6	41.8	10.9	−7.2	−24.4	39.3	64.7	28.3	65.5	4.0	4.3
3/26/98–4/14/98	480	1.4	0.4	100.7	34.0	7.3	−9.6	−14.6	21.3	35.7	7.6	23.7	3.5	3.3
4/14/98–5/14/98	744	1.3	−11.8	89.9	35.1	19.3	−13.4	−41.7	66.7	69.4	65.1	72.1	5.1	2.4
5/30/98–6/25/98	648	2.6	25.0	123.6	17.9	9.6	2.6	40.3	84.1	189.0	31.6	196.0	3.9	2.5
7/10/98–8/13/98	840	1.6	−1.4	112.9	39.3	1.5	23.9	1.7	244.3	226.3	360.2	312.2	7.8	12.0
12/7/98–12/26/98	480	1.4	44.3	233.7	37.0	6.2	49.6	223.5	68.0	822.1	66.0	307.5	2.3	5.5
1/1/99–2/10/99	984	1.3	−21.0	110.6	43.0	15.4	−4.7	−25.9	77.8	63.9	82.9	34.8	4.8	1.5
2/23/99–3/25/99	744	1.0	−49.3	120.1	59.5	10.1	−4.2	−51.0	24.8	46.8	18.2	49.5	4.5	8.8
4/25/99–5/18/99	576	1.3	10.8	114.7	24.4	5.1	14.0	28.7	110.6	170.9	48.6	89.2	1.7	2.5
6/23/99–7/7/99	360	1.7	−28.2	120.1	31.6	5.1	43.9	40.0	199.3	69.7	160.7	45.6	3.3	3.3
8/21/99–8/30/99	240	3.9	−22.3	74.0	42.9	0.9	581.7	245.7	2,286.9	1,120.2	1,878.1	936.6	0.0	1.0
2/8/00–2/26/00	456	1.2	−17.5	115.2	48.3	5.2	−6.2	−28.5	41.2	80.95	14.5	35.2	1.0	0.7
3/31/00–5/6/00	888	1.3	−14.5	131.0	36.3	10.9	−24.0	−45.0	43.7	100.9	21.6	204.2	3.6	5.4
5/22/00–5/30/00	216	3.0	11.9	170.7	24.5	28.6	4.9	38.2	43.4	132.0	34.5	137.4	2.0	1.6
12/15/00–12/22/00	192	1.8	13.4	74.8	23.7	11.1	20.6	29.9	26.9	53.0	0.7	2.8	1.0	1.0
3/12/01–3/30/01	457	1.1	−25.4	64.2	31.4	7.9	−6.6	−33.1	35.9	44.3	50.9	8.4	1.5	1.0
7/26/01–8/1/01	168	1.8	−11.6	204.0	42.6	1.5	156.5	−17.7	336.1	45.9	1185.2	1.1	2.0	0.0
Combined	10,945	1.4	−7.6	139.4	38.0	11.3	−4.4	−15.6	82.1	149.6	110.0	107.9	3.8	3.8
Maximum	984	3.9	44.3	233.7	63.3	33.8	581.7	246.3	2,286.9	1,120.2	1,878.1	936.6	8.0	12.0
Minimum	168	0.7	−49.3	62.2	17.9	0.9	−28.7	−65.9	21.3	35.7	0.7	1.1	0.0	0.0

Table 5. Statistical Parameters: Jamestown

		Precipitation				Streamflow								
							B_v (%)		RMSD (%)		MNPE (%)		MPTE (h)	
Period	Hours	$\overline{G}$ (mm/h)	B_p (%)	RMSD (%)	$P(G>0$ and $R=0)$	$\overline{Q_o}$ (m^3/s)	G	R	G	R	G	R	G	R
2/24/97–3/10/97	360	2.4	−40.2	67.0	26.3	72.4	11.2	−47.8	67.3	113.2	35.6	55.9	1.5	3.8
5/30/97–6/19/97	504	1.3	−31.7	102.2	28.4	33.2	0.9	−14.0	51.1	41.5	33.5	17.7	4.1	5.8
1/1/98–1/20/98	480	1.3	−21.5	115.4	47.6	45.8	−20.1	−39.6	102.4	111.6	51.0	52.4	6.3	5.0
2/1/98–2/26/98	624	0.7	−37.1	77.2	55.9	31.1	−34.9	−57.8	40.4	45.9	36.5	27.2	8.3	9.5
3/6/98–3/26/98	504	1.3	−18.2	67.3	43.2	25.6	−10.5	−27.1	31.1	43.0	36.3	54.7	6.3	9.3
3/26/98–4/14/98	480	1.3	−17.1	86.8	36.8	14.7	−16.9	−31.4	24.1	28.0	25.0	27.8	6.0	5.5
4/14/98–5/14/98	744	1.4	−11.2	101.9	31.1	39.2	−10.2	−30.7	44.6	59.4	35.7	83.8	5.0	5.0
5/30/98–6/25/98	648	2.5	6.5	81.6	17.2	22.1	8.2	19.5	69.5	80.5	45.1	79.9	4.2	6.0
7/10/98–8/13/98	840	1.4	7.5	150.4	27.5	4.0	11.4	9.8	112.6	118.9	105.3	134.4	10.5	13.3
12/7/98–12/26/98	480	1.5	10.8	128.8	33.3	18.2	51.3	45.2	137.7	125.2	346.0	183.9	5.3	6.8
1/1/99–2/10/99	984	1.3	−19.7	97.3	39.8	31.7	−5.3	−27.4	52.5	86.0	27.1	39.7	5.7	7.0
2/23/99–3/25/99	744	1.0	−42.5	99.3	46.0	24.0	−4.9	−49.4	38.7	66.3	27.7	37.5	4.0	5.0
4/25/99–5/18/99	576	1.3	0.2	103.8	26.3	15.6	−0.5	2.4	54.9	62.5	7.5	17.6	9.5	9.5
6/23/99–7/7/99	360	1.8	−3.7	85.3	21.3	25.1	2.3	0.8	94.0	99.2	77.1	67.8	3.2	5.0
8/21/99–8/30/99	240	3.6	−16.9	64.5	20.0	2.3	400.0	156.4	1,218.5	552.0	699.0	302.1	4.0	4.0
2/8/00–2/26/00	456	1.3	−10.5	105.4	40.7	13.6	−4.3	−27.2	38.4	70.4	23.2	17.8	3.7	4.7
3/31/00–5/6/00	888	1.2	−7.9	136.3	36.4	26.2	−30.8	−42.6	58.6	81.4	71.6	112.5	5.2	6.4
5/22/00–5/30/00	216	2.4	−10.4	129.1	17.4	15.1	48.6	16.7	79.5	45.8	82.2	33.9	7.0	5.0
12/15/00–12/22/00	192	2.1	−4.2	63.1	27.0	25.9	−1.4	11.7	28.6	56.3	0.5	0.6	1.0	1.0
3/12/01–3/30/01	457	1.0	−24.9	78.2	40.0	12.3	−13.9	−41.2	33.7	37.1	40.3	11.6	2.0	3.5
7/26/01–8/1/01	168	1.5	−22.1	102.7	36.4	2.2	32.2	−28.8	44.8	26.5	36.8	20.8	2.0	1.0
Combined	10,945	1.4	−14.1	106.6	34.8	23.8	−3.7	−26.5	79.5	105.1	66.2	63.9	5.1	6.0
Maximum	984	3.6	10.8	150.4	55.9	72.4	400.0	156.4	1,218.5	552	699.0	302.1	10.5	13.3
Minimum	168	0.7	−42.5	63.1	17.2	2.2	−34.9	−57.8	24.1	26.5	0.5	0.6	1.0	1.0

maximum depths of each storage zone, the maximum infiltration rate, and the percolation rate are required to simulate the movement of water through the storage zones. Besides precipitation, the only other input for the SMA algorithm is the evapotranspiration rate. A monthly average method is currently the only option for simulating evapotranspiration in HMS (HEC 2000). Seven of the 12 parameters needed for the SMA algorithm (canopy storage, surface depression storage, maximum infiltration rate, maximum soil storage, tension zone storage, soil zone percolation rate, and groundwater-1 percolation rate) were estimated by the processing of land use land cover (LULC) and state soil geographic (STATSGO) database information using a geographic information system (GIS) (Fleming and Neary 2004). Four of the parameters (groundwater-1 and -2 storage depths and storage coefficients) were initially estimated by streamflow recession analysis. The groundwater-2 percolation rate, the only parameter not estimated by physical means (and therefore entirely conceptual), was determined solely through model calibration. Of the physically based parameters, Fleming and Neary (2004) adjusted the tension zone depth and the groundwater storage depths and storage coefficients during model calibration.

For this study, 10 model parameter settings established by Fleming and Neary (2004) were retained. Only the tension zone depth and groundwater-2 percolation rate were adjusted for each of the 21 events and for each precipitation product. In addition, the initial moisture in the soil storage zone was adjusted for each simulation. During model calibration, the tension zone depth was adjusted to match dominant peak flows and the groundwater-2 percolation rate was adjusted to match volumes. The automatic calibration option in HMS was used minimally due to parameter interactions between the tension zone depth and the initial soil storage. When manually calibrating the model, limits were placed on all three adjusted parameters to prevent unreasonable parameter values.

In order to quantitatively compare the hydrologic simulations of BAR and BAG products some common performance statistics were used. The statistics, defined as follows, include streamflow volume bias B_v, relative root mean square difference RMSD, mean normalized peak error MNPE, and mean peak timing error MPTE:

$$B_v(\%) = \frac{\sum_i^n Q_{si} - \sum_i^n Q_{oi}}{\sum_i^n Q_{oi}} \cdot 100 \tag{3}$$

$$\mathrm{RMSD}(\%) = \frac{\sqrt{\frac{1}{n}\sum \Sigma_i^n (Q_{si} - Q_{oi})^2}}{\frac{1}{n}\sum_i^n Q_{oi}} \cdot 100 \tag{4}$$

$$\mathrm{MNPE}(\%) = \frac{1}{n_p}\sum_j^{n_p} \left| \frac{(Q_{sj}^{\max} - Q_{oj}^{\max})}{Q_{oj}^{\max}} \right| \cdot 100 \tag{5}$$

$$\mathrm{MPTE(h)} = \frac{1}{n_p}\sum_j^{n_p} |T_{sj}^{\max} - T_{oj}^{\max}| \tag{6}$$

where Q_s and Q_o=simulated and observed flows, respectively; $Q_s^{\max}$ and $Q_o^{\max}$=simulated and observed maximum flows, respectively; $T_s^{\max}$ and $T_o^{\max}$=times of occurrence of maximum simu-

lated and observed flows; n=total number of hours in each simulation period; and n_p=number of peaks in each simulation period. The results of the performance statistics are summarized for all 21 events and for each subbasin in Tables 4 and 5.

While B_v measures the overall systematic error in the total streamflow volume, RMSD measures the random error quantified by the differences between the individual simulated and observed flow pairs. The last two statistics, MNPE and MPTE, evaluate the accuracy in reproducing the magnitude and timing of peak flows. To allow an overall comparison across the 21 periods, combined, maximum, and minimum values of the performance statistics were calculated and summarized at the bottom of each table. Combined values of the statistics were calculated by combining all of the 21 simulation periods into one continuous record and hence provide an overall measure of performance.

The statistics indicate a wide range of performance for each precipitation product. B_v and RMSD statistics suggest that the BAG model performs better than the BAR model. For the Jamestown subbasin, the magnitude of the B_v statistic for the BAG model is smaller than the BAR model for 15 of the 21 simulation periods. The magnitude of the RMSD statistic for the BAG model is smaller than the BAR model for 16 of the 21 simulation periods. For the Byrdstown subbasin, this is the case for 16 of the 21 simulation periods for the B_v statistic, and 14 of the 21 simulation periods for the RMSD statistic. In addition, the magnitudes of the combined B_v and RMSD values for both subbasins are smaller for the BAG model. For the Jamestown subbasin, the B_v value for the BAG model is -3.7% versus -26.5% for the BAR model. The RMSD value for this subbasin is 79.5% versus 105.1%. For the Byrdstown subbasin, the B_v value is -4.4% versus -15.6%. The RMSD value for this subbasin is 82.1% versus 149.6%.

Both models exhibit an overall underbias in streamflow volume based on the combined B_v values in each subbasin, but the underbias is larger for the BAR model. The larger underbias reflects the radar's underbias in its precipitation estimate despite the recalibration of the BAR model. As discussed by Johnson et al. (1999), the underbias in the streamflow volume lags the underbias in the precipitation estimate. The underbias in the precipitation estimates can also cause additional underbias in streamflow volume for later floods due to the reduced antecedent soil moisture modeled by the SMA algorithm. Conversely, overbias in precipitation estimates can cause additional overbias in streamflow volume for later floods due to increased antecedent soil moisture.

Based on the combined MNPE and MPTE statistics, the BAR and BAG models perform about the same at predicting the magnitude and timing of the peak. For the Jamestown subbasin, the combined MNPE statistics for the BAG model is 66.2% versus 63.9% for the BAR model. For the Byrdstown subbasin, the combined MNPE statistics are also close, 110.0% for the BAG model versus 107.9% for the BAR model. The combined MPTE statistics for both models are also very comparable. For the Jamestown subbasin, the combined MPTE statistic for the BAG model is 5.1 h as compared to 6.0 h for the BAR model. For the Byrdstown subbasin, the combined MPTE statistics are identical, at 3.8 h.

Seasonal trends in performance are also observed. Both models perform poorly for the summer simulation periods when the average flow $\overline{Q_o}$ is very low (e.g., the periods 8/21/99–8/30/99 and 7/26/01–8/1/01). Indeed, the maximum value for B_v, RMSD, and MNPE is observed for both models, and both subbasins, during the period 8/21/99–8/30/99. However, eliminating the poor statistics for this period was found to have a negligible effect on the combined statistics. Notably, the BAR model does

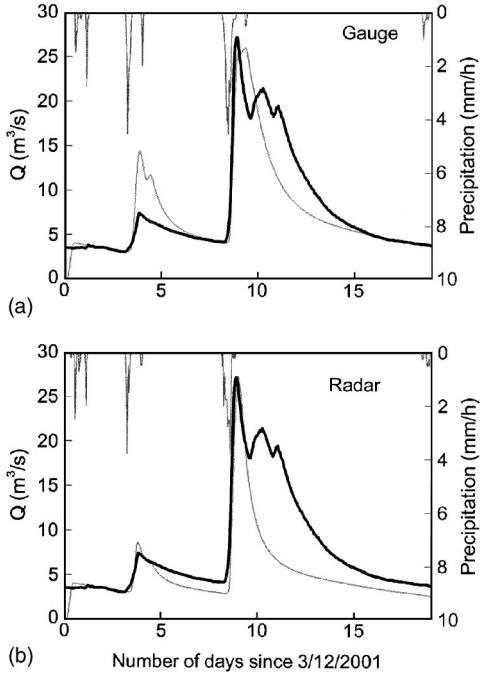

Fig. 3. Measured and simulated streamflow hydrographs for Byrdstown using precipitation data from: (a) Gauge; (b) Radar, March 2001. The thick dark line represents observed streamflow. The thin light line represents simulated streamflow. Hourly precipitation data are also shown.

better than the BAG model for these periods. The poor performance of conceptual hydrologic models for the dry watershed conditions occurring during summer months is not surprising and has been attributed to problems with the model structure (Gan et al. 1997).

In addition to comparing the statistics of BAG and BAR simulations, simulated streamflows were visually evaluated. Examples of the simulated and observed streamflows are shown in Figs. 3–6 for two simulation periods: a Spring 2001 period spanning 3/12/01–3/30/01, and a Spring 1997 period spanning 5/30/97–6/19/97. Statistics for these simulation periods are fairly representative of the overall trends reflected in the combined B_v and RMSD statistics, which indicate better performance by the BAG model. However, the BAR model generally performs better than the BAG model at predicting the magnitude and timing of the peaks during these periods, as reflected in the MNPE and MPTE statistics. Comparing simulated and observed streamflows for both the Spring 1997 and Spring 2001 periods in Figs. 3–6 indicates that neither model performs particularly well. There is significant disagreement between simulated and observed peaks, particularly for the BAG model simulation. Both models fail to predict the last two flood peaks observed for the Byrdstown subbasin during the Spring 2001 event due to the absence of any discernible precipitation input (Fig. 3). Surprisingly both models also fail to resolve the last observed flood peak for the Spring 1997 event in the Byrdstown subbasin even when significant precipitation is detected (Fig. 5). This failure may indicate a potential problem with the SMA algorithm in the HEC-HMS model to ''dry out'' to the point that direct runoff cannot be generated. However, it was found that this last peak could not be simulated even after setting the infiltration rate to zero, which indicates that the radar precipitation was still significantly underbiased. The streamflow plots also illustrate the limitations when considering only a lim-

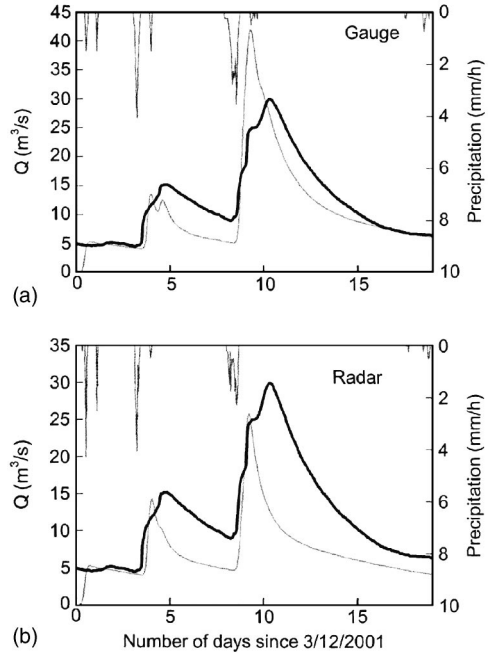

Fig. 4. Measured and simulated streamflow hydrographs for Jamestown using precipitation data from: (a) Gauge and (b) radar, March 2001. The thick dark line represents observed streamflow. The thin light line represents simulated streamflow. Hourly precipitation data are also shown.

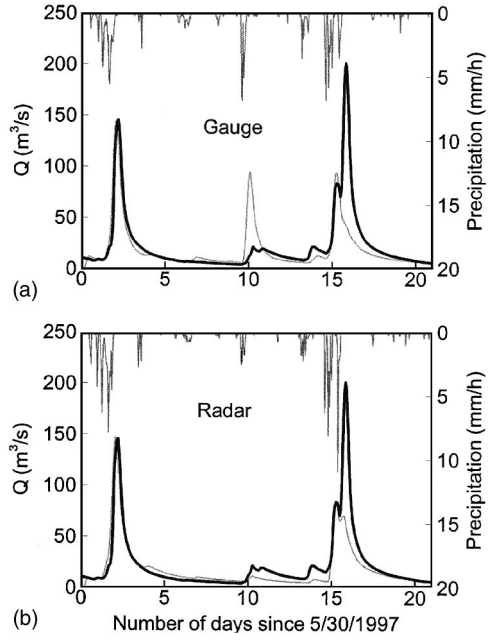

Fig. 5. Measured and simulated streamflow hydrographs for Byrdstown using precipitation data from: (a) Gauge and (b) radar, May–June 1997. The thick dark line represents observed streamflow. The thin light line represents simulated streamflow. Hourly precipitation data are also shown.

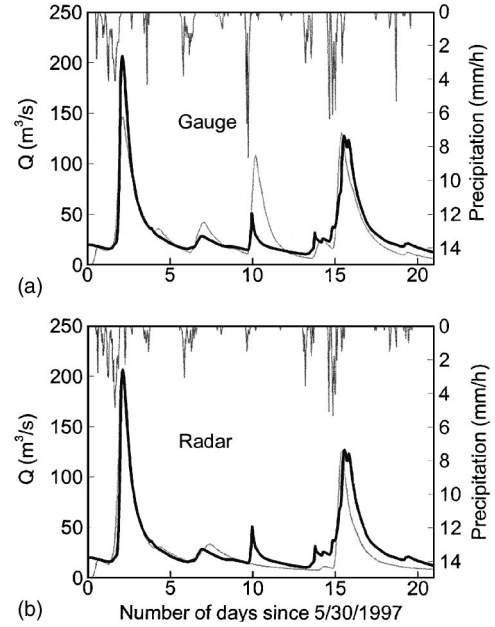

Fig. 6. Measured and simulated streamflow hydrographs for Jamestown using precipitation data from: (a) Gauge and (b) radar, May–June 1997. The thick dark line represents observed streamflow. The thin light line represents simulated streamflow. Hourly precipitation data are also shown.

ited number of summary statistics for evaluating model performance. Although the BAG model exhibits less underbias in streamflow volume overall, as reflected in the B_v statistic, this is partly due to overprediction of flood peaks, as shown in Figs. 3(a)–6(a).

Conclusions

Based on the comparison of gauge and radar data, this study shows that the operational Stage III radar precipitation products suffer from a systematic underestimation of surface precipitation amounts at both point and subbasin scales. In addition, it shows that the radar products are characterized with poor detection capability, especially at low precipitation intensities. Given the fact that in the HEC-HMS simulations the distributed 4×4 km^2 radar data are being averaged over the subbasin areas, it is expected that the most significant improvement in streamflow prediction using radar input would be in streamflow volume. This is masked out by the systematic underbias identified in the radar data. Therefore, serious effort should be directed toward improving the quality of the operational Stage III and removing any systematic bias before utilizing radar data in hydrologic modeling. It is important to note that such efforts are currently being undertaken by the NWS, where new radar products are being developed using the multisensor precipitation estimator (MPE) (Briedenbach and Bradberry 2001). In the new MPE products, estimates from gauges and multiradar sites are optimally merged to produce more accurate precipitation estimates. In particular, the MPE products will have an improved mean-field and local bias correction and are therefore expected to be an improvement over the Stage III products. Future studies should examine the value of the MPE products with HEC-HMS and other continuous hydrologic models.

In addition to radar-related problems, analysis of radar-gauge data also identified some gauge issues that are important for evaluating the accuracy of radar data. A main issue regards the quality of gauge data. Given that gauges represent the most direct means of measuring surface precipitation, it becomes important that their data is of high quality. This can be achieved through careful data collection and special observational setups such as multigauge arrangements where two or more gauges are placed side-by-side (Steiner et al. 1999; Krajewski et al. 2003). Such arrangements will significantly enhance the reliability of the measurements at individual gauge sites. The study also indicates the need for setting up small-scale gauge networks at a few experimental sites within the NEXRAD domains. Such networks would provide accurate representation of areal average precipitation that is necessary in the assessment of radar products. Accurate areal average estimates would also serve as a baseline that can help to distinguish precipitation-related simulation errors from other factors, such as model or parameter estimation uncertainties. Finally, the study emphasizes the importance of having an independent dataset of gauge observations that are not used in the development process of the radar products.

It is important to emphasize that the results of this study are conditioned on the specific hydrologic model used and on the quality of the radar and gauge data used. Conclusions may not be generalized to other watersheds that have different hydrologic and climatologic characteristics. Other factors such as data resolution, spatial and temporal scales, and the quality of the radar products for the region should also be taken into consideration when assessing the results of this study in comparison with other previous studies that addressed the value of radar data for streamflow prediction.

The current study started with the common assumption about the potential improvement of hydrologic simulations by using radar data. The results show that this assumption is not true for the subbasins studied—at least for the case of radar data used with a lumped hydrologic model. Both gauge-only and radar-derived products periodically failed to detect significant precipitation that resulted in observed flood peaks in both subbasins. However, radar-driven HEC-HMS simulations were generally less accurate in prediction of streamflow volume as compared to gauge-driven simulations and, although comparable to the gauge-driven simulations in predicting the magnitude and time to peak, offered no improvement in predicting these quantities either. Interestingly, underbias of the radar precipitation estimates could not be completely offset in the hydrologic model by recalibration; at least when constraining model parameters to realistic limits. It seems reasonable to assume that the performance of the radar-driven hydrologic simulations could be improved further by employing a distributed hydrologic model in conjunction with channel routing so that the full advantage of the radar's ability to provide information on the spatial distribution of precipitation could be gained. A future study that extends the present analysis with a distributed hydrologic model would test this hypothesis.

Acknowledgments

This study was supported by the U.S. Geological Survey and the Nashville District of the U.S. Army Corps of Engineers. The writers thank the reviewers for their constructive comments, which helped to improve the paper.

References

Austin, P. M. (1987). ''Relation between measured radar reflectivity and surface rainfall.'' *Mon. Weather Rev.*, 115, 1053–1070.

Bedient, P. B., Hoblit, B. C., Gladwell, D. C., and Vieux, B. E. (2000). ''NEXRAD radar for flood prediction in Houston.'' *J. Hydrologic Eng.*, 5(3), 269–277.

Beven, K. J., and Hornberger, G. M. (1982). ''Assessing the effect of spatial pattern of precipitation in modeling stream flow hydrographs.'' *Water Resour. Bull.*, 823–829.

Bradley, A. A., and Kruger, A. (1998). ''Recalibration of hydrologic models for use with WSR-88D precipitation estimates.'' *Preprints, Special Symposium on Hydrology; 78th Annual AMS Conf.*, American Meteorological Society, Boston.

Bradley, A. A., Peters-Lidard, C., Nelson, B. R., Smith, J. A., and Young, C. B. (2002). ''Raingage network design using NEXRAD precipitation estimates.'' *J. Am. Water Resour. Assoc.*, 38(5), 1–15.

Brandes, E. A., Vivekanandan, J., and Wilson, J. W. (1999). ''A comparison of radar reflectivity estimates of rainfall from collocated radars.'' *J. Atmos. Ocean. Technol.*, 16, 1264–1272.

Bras, R. L., and Rodriguez-Iturbe, I. (1993). *Random functions and hydrology*, Dover, New York.

Briedenbach, J. P., and Bradberry, J. S. (2001). ''Multisensor precipitation estimates produced by National Weather Service River Forecast Centers for hydrologic applications.'' *Proc., 2001 Georgia Water Resources Conf.*, Institute of Ecology, Univ. of Georgia, Athens, Ga.

Chaubey, I., Haan, C. T., Salisbury, J. M., and Grunwald, S. (1999). ''Quantifying model output uncertainty due to spatial variability of rainfall.'' *J. Am. Water Resour. Assoc.*, 38(5), 1113–1123.

Ciach, J. G., and Krajewski, W. F. (1999). ''On the estimation of radar rainfall error variance.'' *Adv. Water Resour.*, 22(6), 585–595.

Fleming, M., and Neary, V. S. (2004). ''Continuous hydrologic modeling study with HMS.'' *J. Hydrologic Eng.*, 9(3), 175–183.

Fulton, R. A., Breidenbach, J. P., Seo, D.-J., Miller, D. A., and O'Bannon, T. (1998). ''The WSR-88D rainfall algorithm.'' *Weather Forecast.*, 13, 377–395.

Gan, T. Y., Dlamini, E. M., and Biftu, G. F. (1997). ''Effects of model complexity and structure, data quality, and objective functions on hydrologic modeling.'' *J. Hydrol.*, 192, 81–103.

Habib, E., and Krajewski, W. F. (2002). ''Uncertainty analysis of the TRMM ground validation radar-rainfall products: Application to the TEFLUN-B Field Campaign.'' *J. Appl. Meteorol.*, 41(5), 558–572.

Habib, E., Krajewski, W. F., and Ciach, G. J. (2001a). ''Estimation of rainfall interstation correlation.'' *J Hydrometeorol.*, 2, 621–629.

Habib, E., Krajewski, W. F., and Kruger, A. (2001b). ''Sampling errors of tipping-bucket rain gauge measurements.'' *J. Hydrologic Eng.*, 6(2), 159–166.

Habib, E., Krajewski, W. F., Nespor, V., and Kruger, A. (1999). ''Numerical simulation studies of rain gauge data correction due to wind effect.'' *J. Geophys. Res., [Atmos.]*, 104(16), 19723–19734.

Hitch, T. J. (1991). ''Assessment of the adjustment of hourly radar rainfall fields by the use of daily rain gauge totals.'' *Hydrological applications of weather radar*, I. D. Cluckie and C. G. Collier, eds., Ellis Horwood, New York, 49–55.

Hunter, S. (1996). ''WSR-88D radar rainfall estimation: Capabilities, limitations, and potential improvements.'' *NWA Digest*, 20(4), 26–36.

Hydrologic Engineering Center (HEC). (2000). *Hydrologic modeling system HEC-HMS: Technical reference manual*, U.S. Army Corps of Engineers, Davis, Calif.

Johnson, D., Smith, M., Koren, V., and Finnerty, B. (1999). ''Comparing mean areal precipitation estimates from NEXRAD and rain gauge networks.'' *J. Hydrologic Eng.*, 4(2), 117–124.

Krajewski, W. F., Ciach, G. J., and Habib, E. (2003). ''Experimental analyses of small-scale rainfall variability in different climatologic regimes.'' *Hydrol. Sci. J.*, in press.

Krajewski, W. F., Lakshmi, V., Georgakakos, K. P., and Jain, S. C. (1991). ''A Monte-Carlo study of rainfall sampling effect on a distributed catchment model.'' *Water Resour. Res.*, 27(1), 119–128.

Linsley, R. K., Franzini, J. B., Freyberg, D. L., and Tochbanoglous, G. (1992). *Water resources engineering*, 4th Ed., Irwin-McGraw-Hill, New York.

McNutt, J. D., and Neary, V. S. (1999). ''Improvement of basin average rainfall estimates by reducing errors in rain gage and radar data.''

Proc., 1999 Tennessee Water Symp., Nashville, Tenn.
Morrissey, M. L., Maliekal, J. A., Greene, J. S., and Wang, J. (1995). ''The uncertainty of simple spatial averages using rain gauge networks.'' *Water Resour. Res.*, 31(8), 2011–2017.
Obled, C. H., Wendling, J., and Beven, K. (1994). ''The sensitivity of hydrological models to spatial rainfall patterns: an evaluation using observed data.'' *J. Hydrol.*, 159, 305–333.
Ogden, F. L., and Julien, P. Y. (1993). ''Runoff sensitivity to temporal and spatial rainfall variability at runoff plane and small basin scales.'' *Water Resour. Res.*, 29(8), 2589–2597.
Reed, S. M., and Maidment, D. R. (1999). ''Coordinate transformations for using NEXRAD data in GIS-based hydrologic modeling.'' *J. Hydrologic Eng.*, 4(2), 174–182.
Rodriguez-Iturbe, I., and Mejia, J. M. (1974). ''The design of rainfall networks in time and space.'' *Water Resour. Res.*, 10, 713–728.
Seo, D.-J., Breidenbach, J. P., and Johnson, E. R. (1999). ''Real-time estimation of mean field bias in radar rainfall data.'' *J. Hydrol.*, 223, 131–147.
Seo, D.-J., Fulton, R. A., and Breidenbach, J. P. (1997). ''Interagency memorandum of understanding among the NEXRAD Program, WSR-88D Operational Support Facility, and the NWS/OH Hydrologic Research Laboratory.'' *Final Rep.*, NWS/OH Hydrologic Research Laboratory, Silver Spring, Md.
Seo, D. J., and Johnson, E. R. (1995). ''The WS-88D Precipitation Subsystem: An overview and a performance evaluation.'' *Proc., 3rd Int. Symp. on Hydrological Applications of Weather Radar*, Sao Paolo, Brazil.
Smith, J. A., Seo, D.-J., Baeck, M. L., and Hudlow, M. D. (1996). ''An intercomparison study of NEXRAD precipitation estimates.'' *Water Resour. Res.*, 32, 2035–2045.
Smith, M., Koren, V., Finnerty, B., and Johnson, D. (1999). ''Distributed modeling: Phase 1 results.'' *NWS Technical Rep. 44*, National Weather Service, Silver Spring, Md.
Stellman, K. M., Fuelberg, H. E., Garza, R., and Mullusky, M. (2001). ''An examination of radar- and rain gauge-derived mean areal precipitation over Georgia watersheds.'' *Weather Forecast.*, 16(1), 133–144.
Steiner, M., Smith, J. A., Burges, S. J., Alonso, C. V., and Darden, R. W. (1999). ''Effect of bias adjustment and rain gauge data quality control on radar rainfall estimation.'' *Water Resour. Res.*, 35, 2487–2503.
Sun, S., Mein, R. G., Keenan, T. D., and Elliott, J. F. (2000). ''Flood estimation using radar and raingauge data.'' *J. Hydrol.*, 239, 4–18.
Super, A. B., and Holroyd, E. W. (1998). ''Snow accumulation algorithm for the WSR-88D: Final report.'' *Rep. R-98-05*, Bureau of Reclamation, Denver.
Wang, D., Smith, M. B., Zhang, Z., Reed, S., and Koren, V. I. (2000). ''Statistical comparison of mean areal precipitation estimates from WSR-88D, operational and historical gage networks.'' *Proc., 15th Conf. on Hydrology; 80th AMS Annual Meeting*, American Meteorological Society, Boston.
Winchell, M., Gupta, H. V., and Sorooshian, S. (1998). ''On the simulation of infiltration- and saturation-excess runoff using radar-based rainfall estimates: Effects of algorithm uncertainty and pixel aggregation.'' *Water Resour. Res.*, 34(10), 2655–2670.
Young, C. B., Bradley, A. A., Krajewski, W. F., Kruger, A., and Morrissey, M. L. (2000). ''Evaluating NEXRAD multisensor precipitation estimates for operational hydrologic forecasting.'' *J Hydrometeorol.*, 1, 241–254.